J|A|C|S
ARTICLES
Published on Web 12/25/2003

# Theoretical Study of the Trapping of the OOH Radical by Coenzyme Q

Joaquín Espinosa-García*

*Contribution from the Departamento de Química Física, Facultad de Ciencias, Universidad de Extremadura, 06071 Badajoz, Spain*

Received August 11, 2003; E-mail: joaquin@unex.es

***Abstract:*** The reactivity of the hydroperoxyl radical with coenzyme Q, as a prototypical chemical reaction involved in biological antioxidant actions, was studied theoretically. Two pathways were analyzed: the hydrogen abstraction reaction from the phenolic hydrogen on the reduced form (ubiquinol), and OOH addition on the oxidized form (ubiquinone). Optimized geometries, harmonic vibrational frequencies, and energies of the stationary points (reactants, intermediate complexes, transition states, and products) for each pathway were calculated at the BHandHLYP/6-31G level of theory. The reaction paths for the two mechanisms were traced independently, and the respective thermal rate constants were calculated using variational transition-state theory with multidimensional small-curvature tunneling. We found that the reactivity of the OOH radical is dominated by the hydrogen abstraction mechanism on ubiquinol, with a rate constant of $5.32 \times 10^5$ $M^{-1}$ $s^{-1}$, at 298 K. This result strongly contrasts with that, also obtained by our group, for the more reactive OH radical, which attacks ubiquinone by an addition mechanism, with a diffusion-controlled rate of $6.25 \times 10^{10}$ $M^{-1}$ $s^{-1}$, at 298 K.

## 1. Introduction

The peroxidation of lipids (LH) is a free radical chain reaction, which yields peroxyl radicals ($LOO^{\bullet}$)[1,2]

$$LH \xrightarrow{O_2} LOO^{\bullet}$$

It is generally accepted that most free radical trapping antioxidants (AH) capture these radicals by a hydrogen abstraction reaction[2]

$$LOO^{\bullet} + AH \rightarrow LOOH + A^{\bullet}$$

where the resultant antioxidant radical $A^{\bullet}$ is expected to be unreactive, to form the corresponding dimer, or to react with another free radical to yield nonradical products.

Chain-breaking reactions are known to be efficient protection against free radical reaction damage. Natural radical-trapping antioxidants such as coenzyme Q (CoQ) and α-tocopherol (α-TOH, vitamin E), which partition in the lipid bilayer, can avoid or at least significantly reduce free radical reaction damage in a lipid environment.[3−6] As a result, they afford efficient antioxidant protection to biological membranes[4,7,8] and to human low-density lipoproteins (LDL).[9−13] In living cells, coenzyme Q functions also as an obligatory chemical intermediate electron carrier in the electron transport chains of mitochondria[14,15] and plasma membranes,[16] and it has been shown that NADH and ascorbic acid play major roles as electron donors for the reduction of oxidized coenzyme Q in mammalian cells.[16,17]

Considerable experimental work has been devoted to the study of the activity of free radical chain-breaking antioxidants on biological systems.[18−27] These studies concluded that the relative antioxidant activities of CoQ versus α-TOH are CoQ > α-TOH in LDL; CoQ < α-TOH in homogeneous solution; and CoQ ≈ α-TOH in aqueous lipid dispersions,[19] and that the oxidized form of CoQ, that is, ubiquinone, has little or no antioxidant activity.[28−30]

(1) Walling, C. *Free Radicals in Solution*; Wiley: New York, 1957.
(2) Ingold, K. U. *Acc. Chem. Res.* **1969**, *2*, 1.
(3) Stocker, R. *Trends Biochem. Sci.* **1999**, *24*, 219.
(4) Ernster, L.; Dallner, G. *Biochim. Biophys. Acta* **1995**, *1271*, 195.
(5) Forsmark-Andrée, P.; Dallner, G.; Ernster, L. *Free Radical Biol. Med.* **1995**, *19*, 749.
(6) Wolf, G. *Nutr. Rev.* **1997**, *55*, 376.
(7) Tokumaru, S.; Ogino, R.; Shiromoto, A.; Iguchi, H.; Kojo, S. *Free Radical Res.* **1997**, *26*, 169.
(8) Pryor, W. A. *Free Radical Biol. Med.* **2000**, *28*, 141.
(9) Mellors, A.; Tappel, A. I. *J. Biol. Chem.* **1966**, *241*, 4353.
(10) Takayanagi, R.; Takashige, K.; Minakami, S. *Biochem. J.* **1980**, *192*, 853.
(11) Marubayashi, S.; Dohi, K.; Yamada, Y.; Kawasaki, T. *Biochim. Biophys. Acta* **1984**, *797*, 1.
(12) Stocker, R.; Bowry, V. W.; Frei, B. *Proc. Natl. Acad. Sci. U.S.A.* **1991**, *88*, 1646.
(13) Mohr, D.; Bowry, V. W.; Stocker, R. *Biochim. Biophys. Acta* **1992**, *1126*, 247.
(14) Zubay, G. *Biochemistry*; Addison-Wesley: Reading, 1983.
(15) Lenaz, G. *FEBS Lett.* **2001**, *509*, 151.
(16) May, J. M. *FASEB J.* **1999**, *13*, 995.
(17) Villalba, J. M.; Navarro, F.; Córdoba, F.; Serrano, A.; Arroyo, A.; Crane, F. L.; Navas, P. *Proc. Natl. Acad. Sci. U.S.A.* **1995**, *92*, 4887.
(18) Barclay, L. R. C.; Vinqvist, M. R.; Mukai, K.; Itoh, S.; Morimoto, H. *J. Org. Chem.* **1993**, *58*, 7416.
(19) Ingold, K. U.; Bowry, V. W.; Stocker, R.; Walling, C. *Proc. Natl. Acad. Sci. U.S.A.* **1993**, *90*, 45.
(20) Foti, M.; Ingold, K. U.; Lusztyk, J. *J. Am. Chem. Soc.* **1994**, *116*, 9440.
(21) Avila, D. V.; Ingold, K. U.; Lusztyk, J.; Green, W. H.; Procopio, D. R. *J. Am. Chem. Soc.* **1995**, *117*, 2929.
(22) Valgimigli, L.; Banks, J. T.; Ingold, K. U.; Lusztyk, J. *J. Am. Chem. Soc.* **1995**, *117*, 9966.
(23) MacFaul, P. A.; Ingold, K. U.; Lusztyk, J. *J. Org. Chem.* **1996**, *61*, 1316.
(24) Nagaoka, S.; Nishioki, Y.; Mukai, K. *Chem. Phys. Lett.* **1998**, *287*, 70.
(25) Heer, M. I. de; Korth, H.-G.; Mulder, P. *J. Org. Chem.* **1999**, *64*, 6969.
(26) Bowry, V. W.; Ingold, K. U. *Acc. Chem. Res.* **1999**, *32*, 27.
(27) Heer, M. I. de; Mulder, P.; Korth, H.-G.; Ingold, K. U.; Lusztyk, J. *J. Am. Chem. Soc.* **2000**, *122*, 2355.


**10.1021/ja037858j CCC: $27.50** 

In a previous paper,[31] we studied theoretically and experimentally for the first time the mechanism and kinetics of the reaction between the hydroxyl radical and CoQ, in both the reduced (ubiquinol) and the oxidized (ubiquinone) forms. We found that the OH radical, one of the most damaging free radicals that can arise in living organisms,[32] attacks CoQ via two mechanisms: hydrogen abstraction from the phenolic hydrogen on the reduced form (ubiquinol), and electrophilic addition on the oxidized form (ubiquinone). We found that the reactivity is dominated by the OH addition mechanism on ubiquinone, by a factor of 100:1, and that it is a very fast reaction, practically diffusion-controlled, $6.25 \times 10^{10}$ $M^{-1}$ $s^{-1}$, with an inverse dependence of the thermal rate constants on temperature and, therefore, a negative activation energy, both theoretically and experimentally.

In the present work, we continue by studying the reactivity of CoQ, which is present in all membranes of mammalian cells,[33] with free radicals, in this case, the hydroperoxyl radical ($HOO^{\bullet}$). As compared with the hydroxyl radical ($HO^{\bullet}$), the hydroperoxyl radical is a relatively nonreactive free radical. It is necessary to note that this significant bioreaction has been neither theoretically nor experimentally described, and its mechanism and kinetics, to the best of our knowledge, have not been analyzed. Will this free radical follow the hydrogen abstraction mechanism on the reduced form (ubiquinol), as do the peroxyl radicals, or the addition mechanism on the oxidized form (ubiquinone), as does the hydroxyl radical?

The aim of this paper is two-fold: first, to propose a mechanism to account for the attack of the hydroperoxyl radical on CoQ, that is, to analyze theoretically the possible pathways, considering separately the oxidized and reduced forms of CoQ; and second, to obtain theoretical kinetics information. In section 2, we describe the theoretical methods and computational details used in this work. Results and discussion are given in section 3, and, finally, conclusions are presented in section 4.

## 2. Methods and Computational Details

**2.1. Electronic Structure Calculations.** Geometries, energies, and first and second energy derivatives of all stationary points were calculated by hybrid density functional theory (DFT) using the Gaussian 98[34] system of programs. Exchange and correlation were treated by the BHandHLYP method, which is based on Becke's half-and-half method[35] and the gradient-corrected correlation functional of Lee, Yang, and Parr,[36] using the 6-31G basis set. The abbreviation used for this level is BHandHLYP/6-31G. This hybrid DFT method gives more accurate barrier heights than other hybrid DFT methods, such as B3LYP and B3P86.[37−40] It has been pointed out in the literature[41] that these methods present little spin contamination in the treatment of free radicals, with calculated $\langle S^2 \rangle$ values very close to the expectation values, that is, 0.75. Note, however, that spin contamination in DFT calculations is not well defined theoretically and should be handled with caution,[42] although it can be expected that the problems associated with spin contamination for energy calculations are less severe in DFT than in ab initio theory.

***Scheme 1***

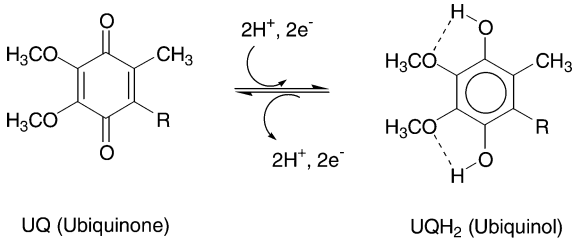


**2.2. Modeling.** Ubiquinone (UQ, oxidized form) and ubiquinol ($UQH_2$, reduced form) are two tautomeric forms of CoQ, related by a two-electron process (Scheme 1),[14] where the number of isoprenoid units can vary from 6 in some yeasts to 10 in humans.[43] Although strictly speaking the denomination coenzyme Q is reserved for the oxidized ubiquinone form, to make the discussion clearer, we will use the denominations ubiquinone (UQ) and ubiquinol ($UQH_2$) for the oxidized and reduced forms, respectively, retaining the name coenzyme Q as a general description of the redox system.

Because of the large size of our molecular system and the great number of calculations (energies, gradients, and Hessians) along the reaction paths, the real biological reaction was modeled in the following way. First, Foti et al.[20] found that the hydrogen abstraction reaction from ubiquinol by phenoxyl radicals is independent of the number of isoprenoid units in the "tail"; that is, practically the same rate constants were found from 0 (ubiquinol-0) to 10 (ubiquinol-10) isoprenoid units. We therefore changed the isoprenoid units in natural $CoQ_{10}$ (see Scheme 1) to a methyl group ($R = -CH_3$). Second, while the theoretical study was performed in the gas phase, given the nonpolar character of the natural environment (lipid bilayer), one can reasonably assume that the conclusions will be roughly the same in both environments. Note that, taking as reference the upper oxygen, the carbon atom positions will be labeled ipso, ortho, meta, and para for a clearer discussion in the following sections.

**2.3. Dynamics Calculations.** The kinetics study of the reaction of CoQ with OOH was carried out using the direct dynamics approach.[44] This describes a chemical reaction by using electronic structure calculations of the energy and energy derivatives (gradients and Hessians) without the intermediary of an analytical potential energy surface or force field. Electronic structure calculations are required only in the region of configuration space lying along the reaction path and

(28) Naumov, V. V.; Khrapova, N. G. *Biofizika* **1983**, *28*, 730.
(29) Yamamoto, Y.; Komouro, E.; Niki, E. *J. Nutr. Sci. Vitaminol.* **1990**, *36*, 505.
(30) Kagan, V.; Serbinova, E.; Packer, L. *Biochem. Biophys. Res. Commun.* **1990**, *169*, 851.
(31) Espinosa-García, J.; Gutiérrez-Merino, C. *J. Phys. Chem. A* **2003**, *107*, 9712.
(32) *CRC Handbook of Methods for Oxygen Radical Research*; Greenwald, R. A., Ed.; CRC Press Inc.: Boca Raton, FL, 1984.
(33) Yamamoto, Y.; Komouro, E.; Niki, E. *J. Nutr. Sci. Vitaminol.* **1990**, *36*, 505.
(34) Frisch, M. J.; Trucks, G. W.; Schlegel, H. B.; Scuseria, E.; Robb, M. A.; Cheeseman, J. R.; Zakrzewski, V. G.; Montgomery, J. A.; Stratman, R. E.; Burant, J. C.; Dapprich, S.; Millam, J. M.; Daniels, A. D.; Kudin, K. N.; Strain, M. C.; Farkas, O.; Tomasi, J.; Barone, V.; Cossi, M.; Cammi, R.; Menucci, B.; Pomelli, C.; Adamo, C.; Clifford, S.; Ochterki, J.; Petterson, G. A.; Ayala, P. Y.; Cui, Q.; Morokuma, K.; Malik, D. K.; Rabuk, A. D.; Raghavachari, K.; Foresman, J. B.; Cioslowski, J.; Ortiz, J. V.; Stefanov, J. J.; Liu, G.; Liashenko, A.; Piskorz, P.; Komaromi, I.; Gomperts, R.; Martin, R. L.; Fox, D. J.; Keith, T.; Al-Laham, M. A.; Peng, C. Y.; Nanayakkara, A.; González, C.; Challacombe, M.; Gill, P. M. W.; Johnson, B. G.; Chen, W.; Wong, M. W.; Andres, J. L.; Head-Gordon, M.; Reploge, E. S.; Pople, J. A. *Gaussian 98*, revision A.7; Gaussian Inc.: Pittsburgh, PA, 1998.
(35) Becke, A. D. *J. Chem. Phys.* **1993**, *98*, 1372.
(36) Lee, C.; Yang, W.; Parr, R. G. *Phys. Rev. B* **1988**, *37*, 785.
(37) Truong, T. N.; Duncan, W. *J. Chem. Phys.* **1994**, *101*, 7403.
(38) Zhang, Q.; Bell, R.; Truong, T. N. *J. Phys. Chem.* **1995**, *99*, 592.
(39) Durant, J. L. *Chem. Phys. Lett.* **1996**, *256*, 595.
(40) Lynch, B. J.; Fast, P. L.; Harris, M.; Truhlar, D. G. *J. Phys. Chem. A* **2000**, *104*, 4811.
(41) Baker, J.; Scheiner, A.; Andzelm, J. *Chem. Phys. Lett.* **1993**, *216*, 380.
(42) (a) Erikson, L. A.; Malkina, O. L.; Malkin, V. G.; Salahub, D. R. *J. Chem. Phys.* **1994**, *100*, 5066. (b) Wang, J.; Becke, A. D.; Smith, V. H. *J. Chem. Phys.* **1995**, *102*, 3477. (c) Laming, G. J.; Handy, N. C.; Amos, R. D. *Mol. Phys.* **1993**, *80*, 1121.
(43) White, A.; Hadler, P.; Smith, E. L. *Biochemistry*; McGraw-Hill: Kogakuska, Tokyo, 1968; p 323.
(44) (a) Doubleday, C. J.; McIver, J. W.; Page, M. *J. Chem. Phys.* **1988**, *92*, 4367. (b) Baldridge, K. M.; Gordon, M. S.; Steckler, R.; Truhlar, D. G. *J. Phys. Chem.* **1989**, *93*, 5107.

the reaction valley formed by the motion orthogonal to it. This method of constructing the potential energy surface has already been used by our group to study smaller systems, in hydrogen abstraction[45−52]and addition reactions,[53] and also in our previous work on the CoQ and OH reaction,[31] with excellent results.

For both pathways independently − hydrogen abstraction on the reduced form (ubiquinol) and addition on the oxidized form (ubiquinone) − we constructed the respective "intrinsic reaction coordinate" (IRC) or "minimum energy path" (MEP) at the BHandHLYP/6-31G level, with a step size of 0.02 bohr amu$^{1/2}$, starting from the respective saddle point geometry and going downhill to both the asymptotic reactant and the product channels in mass-weighted Cartesian coordinates. Along these MEPs, the reaction coordinate, *s*, is defined as the signed distance from the saddle point, with $s > 0$ referring to the product side. In the rest of the work, the units of *s* are bohr, and the reduced mass to scale the coordinates is set to 1 amu. This has no effect on the calculated observables, but it does affect the magnitude of *s* in plots used for interpretative purposes. In this process, one must be careful that electronic structure algorithms do not reorient the molecule. The harmonic vibrational frequencies and reaction-path curvature components were computed at every second point along the reaction path. Along these MEPs, a generalized normal-mode analysis was performed, projecting out frequencies at each point along the path.[54] With this information, we calculated the respective ground-state vibrationally adiabatic potential curves

$$V_a^G(s) = V_{MEP}(s) + \epsilon_{int}^G(s) \quad (1)$$

where $V_{MEP}(s)$ is the classical energy along the MEP with its zero energy at the reactants ($s = -\infty$) and $\epsilon_{int}^G(s)$ is the zero-point energy at *s* from the generalized normal-mode vibrations orthogonal to the reaction coordinate.

Finally, for both pathways (hydrogen abstraction and addition) independently, this information (energies, vibrational frequencies, geometries, and gradients) was used to estimate rate constants by using variational transition state theory (VTST). We calculated thermal rates using the canonical variational theory[55,56] (CVT) approach, which locates the dividing surface between reactants and products at a point $s^{*,CVT}(T)$ along the reaction path that minimizes the generalized TST rate constants, $k^{GT}(T,s)$ for a given temperature *T*. Thermodynamically, this is equivalent to locating the transition state at the maximum $\Delta G^{GT,o}[T, s^{*,CVT}(T)]$ of the free energy of activation profile $\Delta G(T,s)$.[55,56] Thus, the thermal rate constant will be given by

$$K^{CVT}(T) = \sigma(k_B T/h)K^o \exp[-\Delta G(T, s^{*,CVT})/k_B T] \quad (2)$$

with $k_B$ being Boltzmann's constant, *h* Planck's constant, $\sigma$ the symmetry factor, and $K^o$ the reciprocal of the standard-state concentration taken as 1 molecule cm$^{-3}$.

All dynamics calculations were carried out with the general polyatomic rate constant code POLYRATE,[57] and tunneling is included by using the centrifugal-dominant small-curvature tunneling (SCT) approach.[58]

## 3. Results and Discussion

**3.1. Possible Pathways of Attack.** In the biological membrane, both forms of CoQ (ubiquinol, $UQH_2$, and ubiquinone, UQ) are present. To make the discussion clearer, we will distinguish between the attack by the hydroperoxyl radical on the two forms.

**3.1.1. Hydrogen Abstraction Reaction on the Reduced Form.** In this case, the attack of the hydroperoxyl radical on the phenolic O−H of the ubiquinol, $UQH_2$, proceeds via a weakly reactant hydrogen bonded complex (which is denoted HBR), a saddle point (SP), and the products (a "phenoxyl" type radical and water):

$$UQH_2 + OOH \rightarrow HBR \rightarrow SP \rightarrow UQH^{\bullet} + H_2O_2$$

**3.1.1.1. Geometries.** The optimized geometries of reactants, reactant complex, saddle point, and products, using the hybrid DFT BHandHLYP/6-31G level, are shown in Figure 1. There are several geometrical features which will be analyzed following the reaction coordinate, that is, from reactants to products. First, at the four stationary points, all six atoms directly joined to the benzene ring (i.e., two carbons and four oxygens) are in the plane of the ring, favoring electron delocalization. Second, the phenolic hydrogens are hydrogen bonded to the respective oxygens of the neighboring methoxy groups, which favors the stability of the stationary point. The exception is the saddle point, where the hydrogen involved in the breaking−forming bonds is located perpendicular to the benzene plane, losing this possibility. Third, the two methyl substituents of the methoxy groups (ortho- and meta-) are out of the benzene plane in the reactant, one above and the other below. Fourth, another interesting feature is the variation of the C−O distances, because they are related to electron delocalization along the reaction path (Figure 1). Here, for comparison purposes, we take as reference the C−O distances in methanol (single bond character: 1.435 Å) and acetone (double bond character: 1.229 Å) calculated at this same level. The C−O bonds in the ortho-methoxy groups change from 1.391 to 1.371 Å when the reaction evolves from reactants to products. These values are closer to a single bond, although some double bond character is present; that is, they also participate in the electron delocalization. The C−O bond in the phenolic group in position "para" also presents small changes along the reaction path, from 1.379 to 1.359 Å, and shows a greater double bond character. The largest changes are for the C−O bond in the phenolic group directly involved in the hydrogen abstraction, which changes from 1.379 Å in the reactant to 1.296 Å in the ubiquinoxyl radical, showing considerable double bond character. This last behavior agrees with the tendency found for the C−O bond in phenol and the phenoxyl radical from experiment[59,60] or theoretical calcula-

(45) Espinosa-García, J.; Corchado, J. C.; Truhlar, D. G. *J. Am. Chem. Soc.* **1997**, *119*, 9891.
(46) Corchado, J. C.; Espinosa-García, J.; Roberto-Neto, O.; Chang, Y.-Y.; Truhlar, D. G. *J. Phys. Chem.* **1998**, *102*, 4899.
(47) Espinosa-García, J.; Corchado, J. C. *J. Chem. Phys.* **2000**, *112*, 5731.
(48) Corchado, J. C.; Truhlar, D. G.; Espinosa-García, J. *J. Chem. Phys.* **2000**, *112*, 9375.
(49) González-Lafont, A.; Lluch, J. M.; Espinosa-García, J. *J. Phys. Chem. A* **2001**, *105*, 10553.
(50) Espinosa-García, J. *J. Chem. Phys.* **2002**, *116*, 10664.
(51) Espinosa-García, J. *J. Chem. Phys.* **2002**, *117*, 2076.
(52) Espinosa-García, J. *J. Phys. Chem. A* **2003**, *107*, 1618.
(53) Villá, J.; González-Lafont, A.; Lluch, J. M.; Corchado, J. C.; Espinosa-García, J. *J. Chem. Phys.* **1997**, *107*, 7266.
(54) (a) Miller, W. H.; Handy, N. C.; Adams, J. E. *J. Chem. Phys.* **1980**, *72*, 99. (b) Morokuma, K.; Kato, S. In *Potential Energy Surfaces and Dynamics Calculations*; Truhlar, D. G., Ed.; Plenum Publishing: New York, 1981; p 243. (c) Kraka, E.; Dunning, T. H. *Advances in Molecular Electronic Structure Theory*; JAI: New York, 1990; Vol. I, p 129.
(55) Garrett, B. C.; Truhlar, D. G. *J. Am. Chem. Soc.* **1979**, *101*, 4354.
(56) Truhlar, D. G.; Isaacson, A. D.; Garrett, B. C. In *The Theory of Chemical Reaction Dynamics*; Baer, M., Ed.; Chemical Rubber: Boca Raton, FL, 1985; Vol. 4.
(57) Chuang, Y. Y.; Corchado, J. C.; Fast, P. L.; Villá, J.; Coitiño, E. L.; Hu, W. P.; Liu, Y. P.; Lynch, G. C.; Nguyen, K.; Jackells, C. F.; Gu, M. Z.; Rossi, I.; Clayton, S.; Melissas, V.; Steckler, R.; Garrett, B. C.; Isaacson, A. D.; Truhlar, D. G. POLYRATE Version 8.4; University of Minnesota, Minneapolis, 1999.
(58) Lu, D. H.; Truong, T. N.; Melissas, V. S.; Lynch, G. C.; Liu, Y. P.; Garrett, B. C.; Steckler, R.; Isaacson, A. D.; Rai, S. N.; Hancock, G. C.; Lauderdale, G. C.; Joseph, Y.; Truhlar, D. G. *Comput. Chem. Commun.* **1992**, *71*, 235.

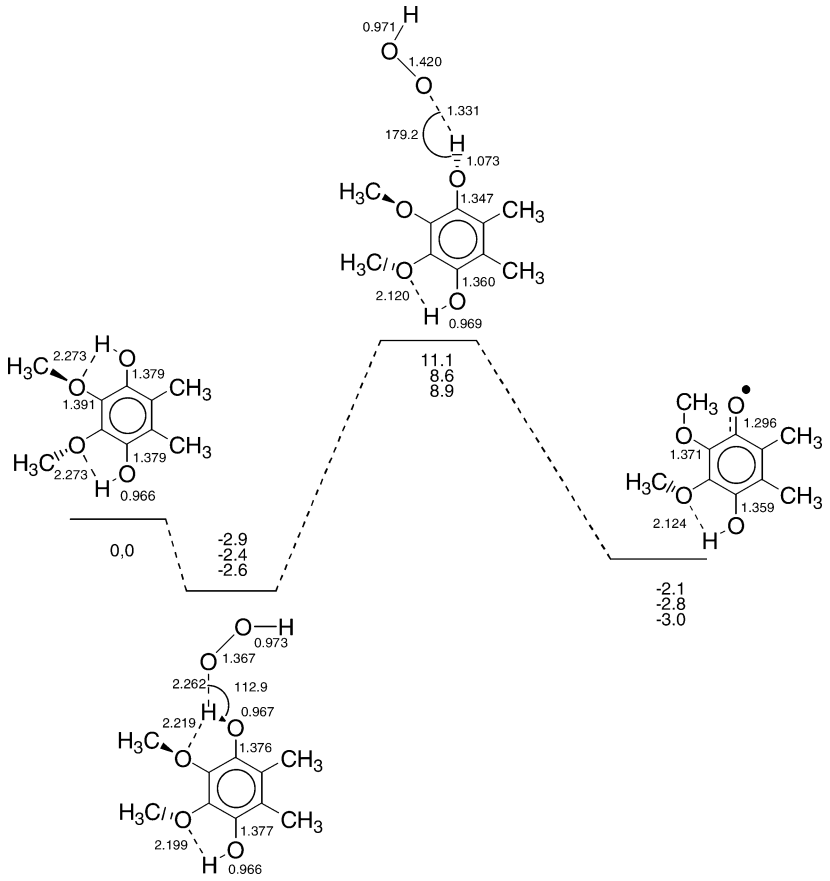


***Figure 1.*** Reaction and barrier height energy and enthalpy at 0 K (second entry) and 298 K (third entry) (kcal mol$^{-1}$) and geometric (bond lengths in angstroms) reaction profile of the OOH + ubiquinol hydrogen abstraction reaction computed at the BHandHLYP/6-31G level of theory.

tions,[61−65] and with the theoretical results for ubiquinol-0,[25] where the C−O bond in position para is 1.367 Å and the C−O bond directly involved in the reaction is 1.258 Å, at the B3LYP/6-31G(d,p) level.

The first stationary point from the reactants is a hydrogen bonded complex (HBR) close to the reactants, with a bond distance (O···$H_1$) of 2.262 Å at this level. The other bond lengths and bond angles are close to those of the separated reactants, and the hydrogen bond formed (O···$H_1$−O) is far from linearity, 112.9°.

Subsequently, a shortening of the O···$H_1$ interatomic distance led us to a second stationary point, which was identified with one negative eigenvalue of the Hessian matrix and, therefore, one imaginary frequency (2188i cm$^{-1}$); that is, it is a saddle point. At this saddle point, the most sensitive parameters are related to the breaking−forming bonds, O(phenolic)−$H_1$ and $H_1$−O(hydroperoxyl). The length of the bond that is broken increases by only 11%, while the length of the bond that is formed increases by 35% with respect to the reactant ($UQH_2$) and product ($H_2O_2$) molecules, respectively. Therefore, the reaction of $UQH_2$ with the hydroperoxyl radical proceeds via an "early" transition state. This is the expected behavior that would follow from Hammond's postulate,[66] because the reaction is exothermic (see Figure 1).

**3.1.1.2. Relative Energies.** Finally, the energy ($\Delta E$) and enthalpy ($\Delta H$, 0 K and 298 K) changes (reaction and activation) are also plotted in Figure 1. Note that $\Delta H$(0 K) is $\Delta E$ corrected by the zero-point energy, and $\Delta H$(298 K) also includes thermal corrections.

We begin by analyzing the heat of reaction. Unfortunately, comparison with experimental or theoretical work is not possible, because the enthalpy of reaction has not been directly measured either experimentally or theoretically. However, an estimate of this value is possible by considering that the enthalpy of reaction, $\Delta H_o°$, is the difference between the bond dissociation energies [BDE(O−H)] of the bonds broken and formed:

$$\Delta H_o° = \mathrm{BDE}(UQH_2) - \mathrm{BDE}(H_2O_2) \qquad (3)$$

Taking BDE($H_2O_2$) = 88.2 ± 1 kcal mol$^{-1}$ and BDE($UQH_2$) = 78.5 ± 1.5 kcal mol$^{-1}$ from the literature,[67,25] a value of $\Delta H_o°$ = −9.7 ± 2.5 kcal mol$^{-1}$ is proposed for the studied reaction (Figure 1). Our result, as in the previous work CoQ + OH,[31] qualitatively describes the exothermic character of this reaction. It is well known that a major source of errors of standard theoretical calculations of molecular energies arises from the truncation of the one-electron basis set. Thus, to estimate the

(59) Larsen, N. W. *J. Mol. Struct.* **1979**, *51*, 175.
(60) Portalone, G.; Schultz, G.; Domenicano, A.; Hargittai, I. *Chem. Phys. Lett.* **1992**, *197*, 482.
(61) Luzhkov, V. B.; Zyubin, A. S. *J. Mol. Struct. (THEOCHEM)* **1988**, *170*, 33.
(62) Chipman, D. M.; Liu, R.; Zhou, X.; Pulay, P. *J. Chem. Phys.* **1994**, *100*, 5023.
(63) Qin, Y.; Wheeler, R. *J. Chem. Phys.* **1995**, *102*, 1689.
(64) Olivella, S.; Solé, A.; García-Raso, A. *J. Phys. Chem.* **1995**, *99*, 10549.
(65) Liu, R.; Morokuma, K.; Mebel, A. M.; Liu, M. C. *J. Phys. Chem.* **1996**, *100*, 9314.
(66) Hammond, G. S. *J. Am. Chem. Soc.* **1955**, *77*, 334.
(67) *JANAF Thermochemical Tables*, 3rd ed.; Chase, M. W., Jr., Davies, C. A., Downey, J. R., Frurip, D. J., McDonald, R. A., Syverud, A. N., Eds.; National Bureau of Standards: Washington, DC, 1985; Vol. 14.

***Table 1.*** Bond Dissociation Energy [BDE(O−H)] for Several Basis Sets at the BHandHLYP Level (kcal mol$^{-1}$)

| basis set | $UQH_2$/UQH | $H_2O_2$/$HO_2$ | $\Delta^a$ | $H_2O$/OH | $\Delta^b$ |
|---|---|---|---|---|---|
| 6-31G | 74.9 | 77.9 | −3.0 | 99.5 | −24.6 |
| 6-31G(d,p) | 78.7 | 79.7 | −1.0 | 107.8 | −29.1 |
| 6-311+G(d,p) | 79.1 | 80.9 | −1.8 | 109.5 | −30.4 |
| 6-311G(2d,2p) | 79.7 | 80.0 | −0.3 | 108.9 | −29.2 |
| exp. | 78.5 ± 1.5[c] | 88.2 ± 1.0[d] | −9.7 ± 2.5 | 117.9 ± 0.1[d] | −39.4 ± 1.5 |

[a] Enthalpy of reaction at 298 K. $\Delta$ = BDE($UQH_2$) − BDE($H_2O_2$). [b] Enthalpy of reaction at 298 K. $\Delta$ = BDE($UQH_2$) − BDE($H_2O$). [c] Reference 25. [d] Reference 67.

limitations, that is, the basis set effect, we performed single-point calculations of the reaction energy and barrier height using larger basis sets, 6-31G(d,p), 6-311+G(d,p), and 6-311G-(2d,2p). For the enthalpy of reaction (298 K), we obtained values of −0.73, −1.75, and −0.29 kcal mol$^{-1}$, respectively. Therefore, for this particular reaction, larger basis sets make the agreement with experiment poorer, indicating that the 6-31G basis set represents a good balance between reactants and products, which makes it adequate to study this reaction. Clearly, it is a question of a fortunate cancelation of errors. It is necessary to note that this behavior of the basis sets strongly contrasts with the results obtained for the similar reaction, CoQ + OH, previously studied by our group,[31] where larger basis sets give better agreement with experiment. To help understand this behavior of the basis sets, we analyze the only experimental magnitude available for comparison, the bond dissociation energy, BDE(O−H). The homolytic BDEs(O−H) involved in both reactions, CoQ + OH and CoQ + OOH, are:

$$UQH_2 \rightarrow UQH + H$$

$$H_2O \rightarrow HO + H$$

$$H_2O_2 \rightarrow HO_2 + H$$

and the corresponding BDEs(O−H) for the different basis sets are listed in Table 1. First, the different BDEs are independently analyzed. The quantum description of the $UQH_2$/UQH pair shows good agreement with the experimental value, even with the smaller basis set, 6-31G. The $H_2O$/OH and $H_2O_2$/$HO_2$ pairs show poor agreement with the experimental data, with differences of 18−9 and 10−8 kcal mol$^{-1}$, respectively. However, the behavior of these two pairs is not similar. Thus, the improvement of the $H_2O$/OH pair with basis set is more pronunced than for the $H_2O_2$/$HO_2$ pair. Second, the enthalpy of reaction, $\Delta$ (obtained as the difference between the BDEs), is analyzed. While the $UQH_2$ + OH reaction agrees better with experiment the larger the basis set is, for the $UQH_2$ + OOH reaction the larger basis sets make this agreement poorer. This behavior agrees with the results obtained for the $H_2O$/OH and $H_2O_2$/$HO_2$ pairs. In sum, the poor quantum description of the $H_2O_2$/$HO_2$ pair with this DFT method explains the basis set effect found for this reaction. Moreover, this analysis justifies the use of the 6-31G basis set in this work.

To estimate the influence of the functional used, we also performed energy calculations of the enthalpy of reaction (298 K) using a different functional, B3LYP. For the 6-31G, 6-31G-(d,p), 6-311+G(d,p), and 6-311G(2d,2p) basis sets, we obtained values of −6.30, −4.51, −5.66, and −3.68 kcal mol$^{-1}$, respectively. With this functional, better agreement with experiment is obtained, but the basis set effect is similar to that found with the BHandHLYP functional; that is, larger basis sets do not yield better agreement with experiment.

***Table 2.*** Barrier Height (kcal mol$^{-1}$) for the $CH_4$ + OH → $CH_3$ + $H_2O$ "Model" Reaction at Several Levels

| level | $\Delta E^{\ddagger}$ | ref |
|---|---|---|
| BHandHLYP/6-31G | 13.4 | this work |
| BHandHLYP/6-31+G(d,p) | 10.2 | 40 |
| B3LYP/6-31+G(d,p) | 2.3 | 40 |
| CBS/QCI/APNO | 5.1 | 68 |
| G2M | 5.3 | 69 |
| CCSD(T)/aug-cc-pVTZ | 5.8 | 70 |
| CCSD(T)-SAC/cc-pVTZ | 5.0 | 71 |

The reactive hydrogen bonded complex (HBR) appears at an energy close to and slightly lower than that of the reactants, −2.9 kcal mol$^{-1}$. When the ZPE (0 K) is included, the stability of the complex slightly diminishes, −2.4 kcal mol$^{-1}$.

Finally, this reaction presents a barrier height ($\Delta E^{\ddagger}$) of 11.1 kcal mol$^{-1}$, and when the ZPE+TC is included the $\Delta H^{\ddagger}$(298 K) is 8.9 kcal mol$^{-1}$. With larger basis sets, 6-31G(d,p), 6-311+G(d,p), and 6-311G(2d,2p), we obtained values of 14.9, 15.8, and 15.9 kcal mol$^{-1}$, respectively (12.8, 13.6, and 13.7 kcal mol$^{-1}$ for the enthalpy (298 K) change), that is, higher than those obtained with the 6-31G basis set. Unfortunately, a direct comparison with experiment is not possible, and given the behavior of these larger basis sets to describe the enthalpy of reaction with errors of 8−9 kcal mol$^{-1}$, larger basis sets do not guarantee a better description of the barrier height for this particular reaction. Also, it is well known that the BHandHLYP level overestimates the barrier heights in hydrogen abstraction reactions,[40] and it has been found empirically that the BHandH-LYP method performs better in calculating barrier heights than other functionals (B3LYP, B3PW91, B3P86, or BLYP) which tend to underestimate them[37−40] due to the creation of an apparent "extra bond" at the transition state.[72] Therefore, based on the previous experience in the literature, the barrier height with the BHandHLYP method has to be diminished. To obtain a more quantitative estimate of the limitations of the BHandH-LYP/6-31G level, we analyzed the "model" hydrogen abstraction reaction $CH_4$ + OH → $CH_3$ + $H_2O$, which has been extensively studied at very high ab initio levels. Note that the more similar $CH_4$ + OOH reaction has not been studied with such high ab initio levels, and therefore comparison would be less interesting. Clearly, this "model" reaction and the title reaction present very different situations, but the observations made with the "model" reaction are assumed to be transferrable to the title reaction as a lower limit. Table 2 lists the most recent results,[40,68−71] together with DFT values for comparison. For the $CH_4$ + OH hydrogen abstraction reaction, when highly correlated wave functions and large basis sets are used (in some cases in combination with extrapolated approaches), the barrier height ranges from 5.0 to 5.8 kcal mol$^{-1}$, with an average value of 5.4 kcal mol$^{-1}$, which is taken as reference. The B3LYP method underestimates this value, in accordance with the general

(68) Malik, D. K.; Petersson, G. A.; Montgomery, J. A. *J. Chem. Phys.* **1998**, *108*, 5704.
(69) Korchowiek, J.; Kawakara, S. I.; Matsumura, K.; Uchimaru, T.; Surgie, M. *J. Phys. Chem. A* **1999**, *103*, 3548.
(70) Aliagas, I.; Gronert, S. J. *J. Phys. Chem. A* **1998**, *102*, 2609.
(71) Masgrau, L.; González-Lafont, A.; Lluch, J. M. *J. Chem. Phys.* **2001**, *114*, 2154.
(72) Tozer, D. J.; Handy, N. C. *J. Phys. Chem. A* **1998**, *102*, 3162.

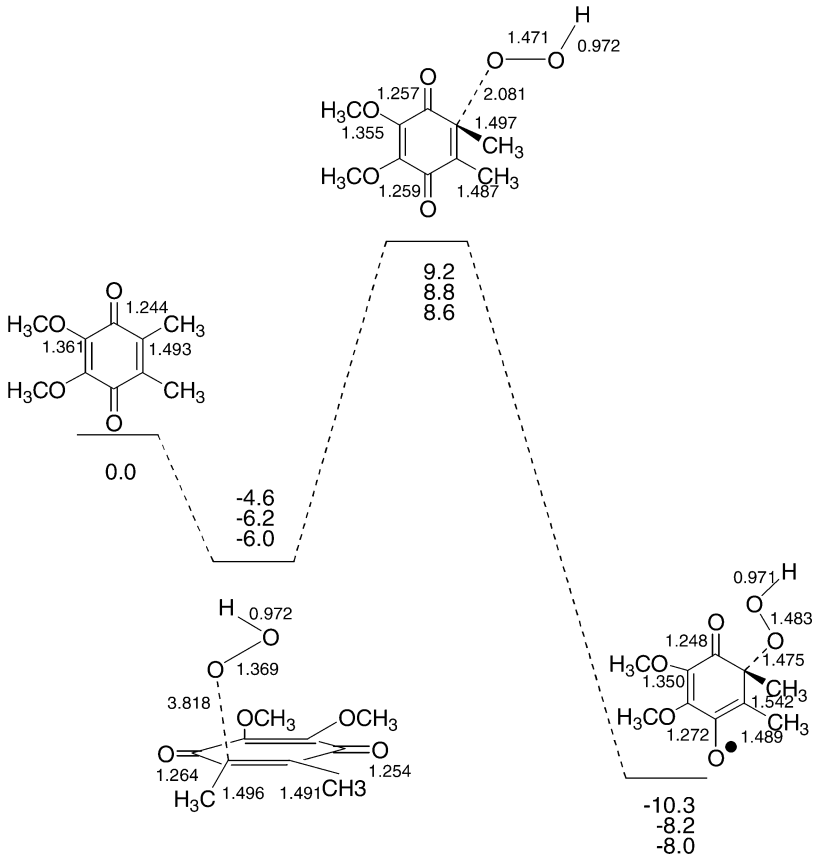


***Figure 2.*** Reaction energy and enthalpy at 0 K (second entry) and 298 K (third entry) (kcal mol$^{-1}$) and geometric (bond lengths in angstroms) reaction profile of the OOH + ubiquinone addition reaction computed at the BHandHLYP/6-31G level of theory.

behavior of the DFT methods, but the BHandHLYP method overestimates it. Fortuitously, at the BHandHLYP/6-31G level both barrier heights, "model" and title reactions, are similar in value. Therefore, to match the very high ab initio average value, the BHandHLYP/6-31G barrier has to be scaled by a factor of 0.4030, which represents a lower limit.

**3.1.2. Addition to Ubiquinone.** In the addition pathway, when the OOH attacks ubiquinone, three approaches are possible: ipso, ortho on $-OCH_3$ (ortho-1), and ortho on $-CH_3$ (ortho-2). Note that, from the symmetry of the modeled system, the other positions (meta and para) are equivalent to those analyzed. The relative energies at the BHandHLYP/6-31G level with respect to the reactants are, respectively, +12.9, −6.6, and −10.3 kcal mol$^{-1}$. Clearly, the ipso approach is unfavorable, and the ortho-2 approach is the most favorable. Therefore, in the rest of the paper, we shall focus on the most favorable approach, although the exothermal nature of the ortho-1 approach means that this will also contribute to the final rate constant. Considering therefore the ortho-2 approach, the attack of the OOH on ubiquinone (UQ) proceeds via a van der Waals complex (vdW), a saddle point (SP), and the adduct product:

$$UQ + OOH \rightarrow vdW \rightarrow SP \rightarrow UQ{-}OOH$$

**3.1.2.1. Geometries.** The optimized geometries of all stationary points (reactants, reactant complex, saddle point, and adduct) and the energy and enthalpy (0 K) changes at the BHandHLYP/6-31G level are shown in Figure 2. Several geometrical features need emphasizing. First, while in ubiquinone all six atoms directly joined to the benzene ring (i.e., two carbons and four oxygens) are in the plane of the ring, the addition of the OOH free radical to form the ortho-2 adduct breaks this planarity on the reactive center. Second, when the OOH attacks ubiquinone, the spin density is located in different oxygen atoms, changing their C−O distances. Thus, on the oxygen it is located in position "para", which changes the C−O distance only slightly, retaining the double bond character. Third, another interesting feature is the value of the new C−O bond formed with the OOH attack, which is weaker than a single bond.

The first stationary point from the reactants is a van der Waals complex. The OOH radical approaches parallel to the molecular plane, with bond distances O−C(ipso), O−C(ortho-1), and O−C(ortho-2) of 3.181, 3.344, and 3.818 Å, respectively. The other geometrical parameters are close to those of the separated reactants. It is well known that DFT is not able to describe intermolecular interactions with any reasonable accuracy,[73−76] and the problem is related to the description of the weak dispersion interaction.[77] However, for the most attractive geometries of the $(H_2O)_2$ hydrogen bond and the $CO{-}H_2O$ van der Waals complex, that is, relatively strong intermolecular interactions, some functionals (B3LYP and B3P86) perform reasonably well.[74] We assume a similar behavior for our van der Waals complex, which presents a relatively strong interaction, −6.0 kcal mol$^{-1}$ at 298 K. More theoretical studies are

(73) Del Bene, J. E.; Person, W. B.; Szczepanik, K. *J. Phys. Chem.* **1995**, *99*, 10705.
(74) Milet, A.; Korona, T.; Moszynski, R.; Kochanski, E. *J. Chem. Phys.* **1999**, *111*, 7727.
(75) Lein, M.; Dobson, J. F.; Gross, E. K. U. *J. Comput. Chem.* **1999**, *20*, 12.
(76) Chalasinski, G.; Szczesniak, M. M. *Chem. Rev.* **2000**, *100*, 4227.
(77) Zaremba, E.; Khon, W. *Phys. Rev.* **1976**, *B13*, 2278; **1977**, *B15*, 1769.

***Table 3.*** Barrier Height (kcal mol$^{-1}$) for the $CH_2{=}CH_2 + OOH \rightarrow (CH_2{=}CH_2){-}OOH$ "Model" Reaction at Several Levels

| level | $\Delta E^{\ddagger}$ | ref |
|---|---|---|
| BHandHLYP/6-31G | 10.5 | this work |
| B3LYP/6-31G(d) | 9.2 | 78 |
| MP2/6-31G(d) | 18.8 | 78 |
| CBS-q//MP2/6-31G(d) | 14.6 | 78 |

clearly necessary to assess the performance of the DFT in describing van der Waals interactions.

Subsequently, a greater approach of the OOH radical led us to a second stationary point, which is characterized as a saddle point (imaginary frequency 280i cm$^{-1}$). The OOH radical is now oriented perpendicular to the molecular plane, with an O−C(ortho-2) distance of 2.081 Å.

**3.1.2.2. Relative Energies.** The energy ($\Delta E$) and enthalpy ($\Delta H$,0 K) changes (reaction and activation) are also plotted in Figure 2. Unfortunately, comparison of these magnitudes with experimental or theoretical work is not possible because there have not been any measurements in either case.

With respect to the barrier height, we will follow a procedure similar to that for the hydrogen abstraction reaction analyzed previously. Thus, to test the accuracy of the BHandHLYP/6-31G level used in this work, we analyzed the "model" addition reaction $CH_2{=}CH_2 + OOH \rightarrow (CH_2{=}CH_2){-}OOH$, which has been studied at high ab initio levels. Table 3 lists these results[78] together with other DFT values for comparison. For the addition reaction to ethylene, the high ab initio CBS-q//MP2(full)/6-31G level yields a barrier of 14.6 kcal mol$^{-1}$, which is taken as reference. In this case, both DFT methods, BHandHLYP and B3LYP, underestimate this value, in accordance with the general behavior of the DFT methods. To match this reference barrier, the BHandHLYP/6-31G value has therefore to be scaled by a factor of 1.3905.

In sum, we have applied the $CH_4 + OH$ and $CH_2{=}CH_2 + OOH$ reactions as test cases of hydrogen abstraction and addition reactions, respectively, to assess the performance of the DFT method used in this work, BHandHLYP/6-31G. The observations made with these "model" reactions are believed to be transferrable also to the larger systems studied in this work: ubiquinol + OOH and ubiquinone + OOH.

**3.2. Reaction-Path Analysis.** Having analyzed the stationary points for the hydrogen abstraction and addition reactions, we next constructed the respective reaction paths independently. The analysis of these reaction paths is carried out on the information (energy, gradient, and Hessian) at the BHandHLYP/6-31G level over the $s$ range −0.5 to +0.5 bohr.

Whereas for the hydrogen abstraction reaction, ubiquinol + OOH, the location of the maximum of $\Delta V_a^G$ practically coincides with the saddle point ($s = 0$), for the addition reaction, ubiquinone + OOH, the location of the maximum of $\Delta V_a^G$ appears shifted with respect to the saddle point, $s = +0.355$ bohr, in the product channel. Therefore, the variational effects are practically negligible for the first reaction and large for the second (a variational effect is the difference between the variational CVT and conventional TST rate constants). Note that $\Delta V_a^G$ is defined as the difference between $V_a^G$ at $s$ and its value for the reactants.

(78) Chen, Ch.-J.; Bozzelli, J. *J. Phys. Chem. A* **2000**, *104*, 4997.

***Table 4.*** Rate Constants for the CoQ + OOH Reaction[a]

| | ubiquinol + OOH | | | | ubiquinone + OOH | | | |
|---|---|---|---|---|---|---|---|---|
| $T$ (K) | TST | CVT | SCT | CVT/SCT | TST | CVT | SCT | CVT/SCT |
| 200 | 7.11(4) | 3.14(4) | 4.87 | 1.53(5) | 8.42(−9) | 3.73(−9) | 1.65 | 6.15(−9) |
| 250 | 2.52(5) | 1.10(5) | 2.75 | 3.02(5) | 6.50(−6) | 3.22(−6) | 1.35 | 4.35(−6) |
| 300 | 6.38(5) | 2.78(5) | 2.01 | 5.58(5) | 5.92(−4) | 3.14(−4) | 1.22 | 3.83(−4) |
| 350 | 1.32(6) | 5.73(5) | 1.67 | 9.57(5) | 1.58(−2) | 8.79(−3) | 1.15 | 1.01(−2) |
| 400 | 2.38(6) | 1.04(6) | 1.48 | 1.54(6) | 1.96(−1) | 1.13(−1) | 1.11 | 1.25(−1) |
| 450 | 3.95(6) | 1.72(6) | 1.36 | 2.34(6) | 1.45(0) | 8.61(−1) | 1.09 | 9.38(−1) |
| 500 | 6.14(6) | 2.66(6) | 1.28 | 3.40(6) | 7.47(0) | 4.50(0) | 1.07 | 4.81(0) |

[a] 7.11(4) stands for $7.11 \times 10^4$, in $M^{-1}$ $s^{-1}$. Values were obtained with the scaled reaction paths.

This different behavior of the variational effects can be explained by analyzing the variation of ZPE with $s$. In the first reaction, as is typical of hydrogen abstraction reactions, the $O{-}H_1$ (phenolic) stretching, corresponding to the generalized normal mode breaking during the reaction (reactive mode), drops sharply near the saddle point, which causes a considerable fall in the ZPE in the saddle point region ($\Delta ZPE = -2.5$ kcal mol$^{-1}$). As a result, the ZPE shows noticeable changes with $s$, and, therefore, variational effects could be expected for this reaction. However, the barrier height is large (11.1 kcal mol$^{-1}$), and thus the energy factor, which locates the generalized transition state at the saddle point ($s = 0$), dominates over the entropy factor ($\Delta ZPE$). For the addition reaction, however, $\Delta ZPE$ is practically constant as $s$ varies, increasing from reactants to the adduct, with a value of only $\Delta ZPE = +0.6$ kcal mol$^{-1}$ at the saddle point. Thus, in the product zone, the ZPE rises, which shifts the maximum of the $\Delta V_a^G$ curve in this direction.

Finally, from an energy point of view, we saw in sections 3.1.1.2 and 3.1.2.2 the poor energy description obtained with the BHandHLYP/6-31G level, which means that we have to optimize our low level reaction path. In previous papers,[79−81] we analyzed different approximations and found that the best choice was to scale the original curve (BHandHLYP/6-31G) regularly by a factor

$$F = \Delta E(\text{reference level}, s{=}0)/\Delta E(\text{BHandHLYP/6-31G}, s{=}0) \quad (4)$$

where $\Delta E$ is the variation of energy at each level with respect to the reactants, and the "reference level" is the best estimate for the respective "model" reaction: $CH_4 + OH$ in the first reaction, and $CH_2{=}CH_2 + OOH$ in the second. Thus, at the saddle point, $s = 0$, the barrier height is that of the respective "reference level". These factors are 0.4030 and 1.3905 for the hydrogen abstraction and addition reactions, respectively.

**3.3. Rate Constants.** In the canonical version of VTST, CVT, the dividing surface is varied along the reaction path to minimize the rate constants, obtaining the generalized transition state (GTS) at the value $s$*. Thermodynamically, the minimum rate constant criterion is equivalent to maximizing the generalized standard state free energy of activation, $\Delta G^{GT,o}(T,s)$, eq 2. Therefore, the effects of the potential energy, entropy, and temperature on the location of this GTS must be considered.

Table 4 lists the calculated conventional TST and variational CVT rate constants for the hydrogen abstraction and addition

(79) Espinosa-García, J.; Corchado, J. C. *J. Chem. Phys.* **1994**, *101*, 8700.
(80) Espinosa-García, J.; Corchado, J. C. *J. Chem. Phys.* **1994**, *101*, 1333.
(81) Espinosa-García, J. *J. Phys. Chem.* **2000**, *104*, 7537.

reactions, together with the tunneling effects, on the scaled reaction paths, over the temperature range 200−500 K. (Note that while this range is very wide for a biological system, it permits a clearer interpretation of the temperature dependence of the rate constants.) The hydrogen abstraction reaction on ubiquinol (reduced form of CoQ) is notably faster than the OOH addition on ubiquinone (oxidized form of CoQ), and the hydrogen abstraction mechanism therefore seems to be the most favorable pathway. Thus, the total rate constants of the OOH + CoQ reaction practically coincide with the hydrogen abstraction values.

The activation energy can be obtained from the total rate constants through the usual definition

$$Ea = -R\, \mathrm{d}(\ln k)/\mathrm{d}(1/T) \qquad (5)$$

which is equivalent to determining the slope of the Arrhenius plot, that is, ln $k$ versus $1/T$. At 298 K, our best estimate is 2.1 kcal mol$^{-1}$.

Finally, with the rate constant obtained in the present work with the OOH radical, in the previous[31] with the OH radical, and from the literature[18,20,27] with other free radicals, we propose the following ranking of the reactivity of CoQ with different free radicals:

$$\mathrm{OH} > \text{alkoxyl}^{27} > \text{phenoxyl}^{20} > \text{peroxyl}^{18} \approx \mathrm{OOH}$$

indicating that the more located the unpaired electron is on the radical center (oxygen atom in these cases), the more reactive it is.

## 4. Concluding Remarks

There has been considerable experimental effort directed at understanding the role of antioxidants in biological processes and cell survival, in contrast with the paucity of theoretical studies. In the present paper, by employing a direct dynamics method, we were able, for the first time, to study the kinetics and dynamics of this antioxidant process using as a prototype reaction that of coenzyme Q with the hydroperoxyl radical in the gas phase.

The OOH radical can attack coenzyme Q by different pathways, and we found that the most favorable mechanisms are the hydrogen abstraction reaction from the phenolic hydrogen on the reduced form (ubiquinol) and OOH addition on the oxidized form (ubiquinone). The equilibrium structures of all stationary points and the reaction valleys for both mechanisms were analyzed using hybrid density functional theory at the BHandHLYP/6-31G level.

The rate constants for each mechanism were calculated independently using the variational transition-state theory with multidimensional tunneling. We found that the hydrogen abstraction reaction on ubiquinol is responsible for the overall rate constant. These final rate constants present a positive temperature dependence, leading to a positive activation energy.

This behavior of the relatively nonreactive OOH radical strongly contrasts with the behavior observed for the highly reactive OH radical.[31] Thus, while the reactivity of the OOH radical is dominated by the hydrogen abstraction mechanism on ubiquinol (reduced form of CoQ) with a rate constant of $5.32 \times 10^5$ M$^{-1}$ s$^{-1}$ at 298 K, the reactivity of the OH radical is dominated by the addition mechanism on ubiquinone (oxidized form of CoQ) with a very fast rate constant, practically diffusion-controlled, of $6.25 \times 10^{10}$ M$^{-1}$ s$^{-1}$ at 298 K. The results obtained with these two studies allow us to understand the antioxidant properties of coenzyme Q, especially important in the case of the very dangerous hydroxyl radicals. This suggests the idea of include CoQ in supplementation therapy.

Finally, it has recently been shown[82−84] that some mutants (clk-1) do not synthesize CoQ, but instead accumulate an intermediate form of CoQ, demethoxyubiquinone (DMQ). The only difference with CoQ is the lack of a methoxy group on carbon six, preventing the interaction with the upper oxygen in ubiquinol. DMQ is capable of carrying out the function of CoQ in the respiratory chain, presents antioxidant properties, and may contribute to the extension of life span.

**Acknowledgment.** We are grateful to Prof. Donald G. Truhlar for providing a copy of the POLYRATE program, to Dr. José C. Corchado for computational support, and to the Consejeria de Educación, Ciencia y Tecnología, Junta de Extremadura (Spain) (Project No. 2PR01A002), for partial financial support of this work.

JA037858J

(82) Miyadera, H.; Amino, H.; Hiraishi, A.; Taka, H.; Murayama, K.; Miyoshi, H.; Sakamoto, K.; Ishii, N.; Hekimi, S., Kita, K. *J. Biol. Chem.* **2001**, *276*, 7713.
(83) Hihi, A. K.; Gao, Y.; Hekimi, S. *J. Biol. Chem.* **2002**, *277*, 2202.
(84) Miyadera, H.; Kano, M.; Miyoshi, H.; Hekimi, S.; Kita, K. *FEBS Lett.* **2002**, *512*, 33.